

## Preparation and characterization study of an olive pomace - polyaniline composite conductor in the recovery of heavy metals by electrosorption and adsorption.

N. Babakhouya<sup>(1,2\*)</sup>, M. Abdouni<sup>(1)</sup>, K. Louhab<sup>(1)</sup>

<sup>1</sup>Food Technology Research Laboratory (LRTA) Faculty of Sciences Engineer  
University of M'hamed Bougara, Boumerdes, BP 70, 35000 Boumerdes-Algeria

<sup>2</sup>Scientific and Technical Research Center of Physico-chemical Analysis, BP 384, Siège ex-  
Pasna Zone Industrielle, Bou-Ismaïl CP 42004, Tipaza, Algérie

\*Corresponding author: nawelamini@yahoo.fr

### ABSTRACT/RESUME

#### Article History:

Received : 05/05/2018

Accepted : 10/07/2018

#### Key Words:

Olive-pomace ;  
Polyaniline ;  
Insitu-polymerization ;  
Hexavalent Chromium ;  
Electrosorption ;  
Adsorption.

**Abstract:** In this work, we have prepared a new composite material based on olive pomace (OP) and polyaniline (PANI) by the in situ-polymerization chemical method, demonstrated the ability of our material to conduct current through electrical conductivity tests. We used the spectral analysis techniques to characterize the material as well as Laser Particle Size and scanning electron microscopy to show that the PANI was successfully attached to OP. We have applied our new material in the recovery of Hexavalent Chromium by carrying out electrosorption tests at a positive potential imposed. We compared the recovery with chemical adsorption under the same conditions.

### I. Introduction

Significant processes were widely studied to eliminate heavy metals, pollutants of waste water in high concentrations [1,2] resulting in a remarkable improvement in water quality. Some of these processes are: coagulation and flocculation, floatation, membrane process, adsorption and chemical and electrochemical oxidation processes. Among these techniques adsorption has been shown to be an effective process with its applicability on a large scale to remove impurities from waste waters. However, time required for adsorption is sometimes long [3]. On the other hand electrosorption; which is generally defined as potential-induced adsorption of molecules on the surface of charged electrodes is promising technology for faster and more effective removal of pollutants from waste water [4,5]. In this respect, electrosorption offers some advantages such as its environmental friendliness, and the in-situ regeneration of adsorbent with less energy consumption, [6,7]. Diverse materials as cellulose,

rubber, and textile were used as good supports for the electrosorption because of their distinguished physical properties. Nevertheless, we have selected a new material not used yet in this area, namely the olive pomace. Olive pomace is one of the most abundant materials in nature; it possesses several advantages such as low cost, low density, non-toxicity, renewable nature, biodegradability [8]. It was been reported to be a suitable adsorbent material [9]. However, to achieve an electrosorption with natural material, we must make it conductive. To this end the conductive polymer is used. In terms of conductive polymers, polyaniline (PANI) is extensively studied conjugated polymer with particular properties such as good environmental stability, high electrical conductivity, ease of preparation, low synthesis cost and reversible acid/base doping/dedoping characteristics [10,11]. The main objective of this work is to fabricate a composite based on olive pomace, to make it conductive and to study its applicability in the

electro-enhanced removal of chromium hexavalent from aqueous solution.

## II. Experimental

### II.1. Materials and methods

The olive pomace results from seeds crushed during the production process of the olive oil. They are washed at first several times in the tap water then in the distilled water subsequently, exhausted by the hexane to eliminate the residual oil, washed with some hot distilled water, dried and crushed in a diameter between 500  $\mu$  and 1000  $\mu$  [12]. The chemicals we have used to produce our samples such as Aniline monomer and Ammonium persulfate (APS) have been purchased from Biochem Chemopharma Inc. and the Hydrochloric acid (HCl) from Chem-lab Inc.

### II.2. Synthesis of olive pomace–PANI composites

We have considered two grams (2g) quantity of olive pomace in the preparation of the composites samples according to the In situ polymerization process. We added to this quantity 2.0 mol/L of HCl solution dissolving aniline monomer (10:1 by molar ratio), stirred for 50 minutes, then added 0.025 mol/L of APS aqueous solution drop wise to oxidative polymerize aniline [13]. The mixture was stirred for 20 hours at room temperature [14]. The reaction product was filtrated and washed with 0.2 mol/l of chloride acid solution [15], and then with absolute ethanol till the filtrate become colorless. Finally, the composites were dried at 40 °C in an air oven for 5 hours. We have produced with the same process described earlier six samples by progressively increasing the aniline, HCL, and the persulfate as shown in table 1 below.

**Table 1.** Samples prepared by In situ polymerization

Samples	Amount of aniline (mmole)	Amount of HCL (mmole)	Amount of Persulfate Ammonium APS (mmole)	Amount of olive pomace (g)
1	2	20	2.5	2
2	4	40	5	2
3	8	80	10	2
4	12	120	15	2
5	16	160	20	2
6	20	200	25	2

### II.3. Characterization

We have applied the Fourier transform infrared spectra (FT-IR) to the samples using the EQUINOX-55 FT-IR spectrometer (Bruker laser) and recorded

the Spectra in the range 4000–400  $\text{cm}^{-1}$ . As well as the DMAX-Ultima III X-ray diffractometer in the range from 5° to 120° to obtain the X-ray diffraction (XRD) results of the composites. Furthermore, the size distribution of PANI nanoparticles in olive pomace was analyzed by using Gatan Digital Micrograph software. Finally, scanning electron microscopy (Philips ESEM XL 30 SEM, JEOL, Inc., JSM- 6500F) was used to characterize the surface morphology and structure of the samples. The electrical conductivity (EC) of the composites was measured at room temperature by the standard four-probe method. The samples were compressed to 13 mm diameter and 0.08–0.2 mm thickness pellets for the measurements.

## III. Results and discussion

### III.1. Structure and morphology analysis

#### III.1.1. FT-IR characterization

The FT- IR spectra of olive pomace (1), PANI-HCl (2) and olive pomace – PANI composite (3) are shown in Fig1. The characteristic broad band for O–H group (being in presence of H-bond) of olive pomace appears at 3330  $\text{cm}^{-1}$  [16,17,18], a peak around 1730  $\text{cm}^{-1}$  due to functional group C=O of lactones [16] and the band 1234  $\text{cm}^{-1}$  corresponds to the vibrations of the function OH and NO<sub>2</sub>. So the band 1031  $\text{cm}^{-1}$  indicates the presence of the connections of strain C- OH primary alcohol and C-N. The broad absorption band between 1200 and 935  $\text{cm}^{-1}$  is attributed to the contribution of various functional groups, such as C–O and C–O–C. The typical feature of pure PANI is also well known in literature. The peaks corresponding to out of bending vibration of N–H and C–H band of p-di-substituted benzene appears at 497  $\text{cm}^{-1}$  and 790  $\text{cm}^{-1}$ . The band 1079  $\text{cm}^{-1}$  indicates the presence of the connections of strain C- OH primary alcohol and C-N. The 1278  $\text{cm}^{-1}$  band corresponds to an NH bending out of plane and stretching vibrations of C–O phenolic bond and C–N on the benzoide cycle [18]. The peaks around 1457 and 1557  $\text{cm}^{-1}$  result from stretching vibration of N–A–N and N=B=N structures, respectively (where –A– and =B= stand for benzenoid and quinoid moieties in the PANI chains) [19,20]. The 1780  $\text{cm}^{-1}$  band is characteristic of the conducting form of PANI. The characteristic absorptions of pure cellulose (3331, 1234 and 1031  $\text{cm}^{-1}$ ) and PANI (1780, 1557, 1457 and 1278  $\text{cm}^{-1}$ ) have been both present in the spectrum of the composite [15].

The FT-IR spectrum of OP/PANI indicates that the composing of OP and PANI is successful.

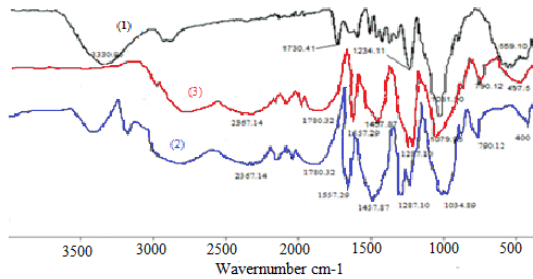


Figure 1. FT-IR spectra of olive pomace (1), PANI-HCl (2) and OP/PANI-HCl composite with 39,42% of PANI (3).

### III.1.2. X-ray diffraction characterization

Figure 2 shows XRD patterns of pure olive stone, PANI-HCl and OP/PANI-HCl composite. The diffractogram of olive pomace exhibits a crystalline major peak at  $2\theta = 22.4^\circ$  [21,22], corresponding to the (200) crystallographic plane which is attributed to typical cellulose I structure also called native cellulose constituting the crystalline part of cellulose [23,24]. The other constituents of olive pomace are predominantly amorphous which is explained by the appearance of the spectrum from  $2\theta = 22.4^\circ$ . For the plane PANI, the major diffraction peaks at  $2\theta = 18.5^\circ$ ,  $18.6^\circ$  and  $25.2^\circ$  are consistent with (020) and (200) crystal planes respectively [25,26]. Similar to the PANI prepared by conventional methods [8], the peaks of our PANI  $2\theta = 18.5^\circ$ ,  $18.6^\circ$  and  $25.2^\circ$  are ascribed to the periodicity parallel and perpendicular to the polymer chains of PANI respectively, which indicates that PANI is partially crystalline as previously reported [8]. This crystallinity is also dependent on the acid used for synthesis and the degree of doping [27]. However XRD of OP/PANI-HCl composite reveals broad diffraction peaks typical to those obtained from the pure PANI (at  $2\theta = 25.51^\circ$ ) and the pure olive pomace (at  $2\theta = 22.28^\circ$ ) indicating a successful coating of PANI over olive pomace [27]. From the graph, the emergence of an additional peak at  $15.87^\circ$  corresponds to the orientation (010) [28].

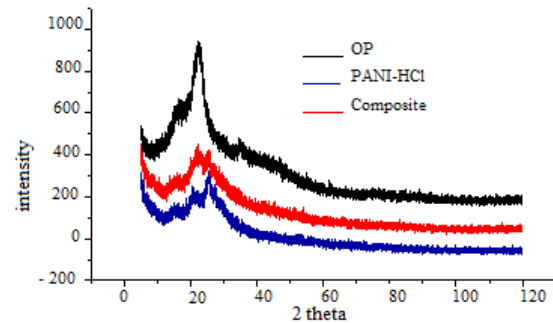


Figure 2. X-ray diffraction patterns of olive pomace, PANI and OP/PANI composite with 39,42% of PANI.

### III.1.3. Characterization by Laser granulometry

Figures 3.a, 3.b and 3.c show respectively the size distribution of OP, PANI and OP/PANI composite distribution of the particle size in olive pomace located around  $24,315 \mu\text{m}$  for a volume of 50%. From the PANI-HCl, the particle size repartition was located around  $9,802 \mu\text{m}$  for 50% of the samples. However, for the OP/PANI composite, the size distribution was  $40,668 \mu\text{m}$  to 50% of the samples. After mixing, we notice an increase in particle size, which will allow us to say that there were agglomeration between particles of olive pomace and PANI.

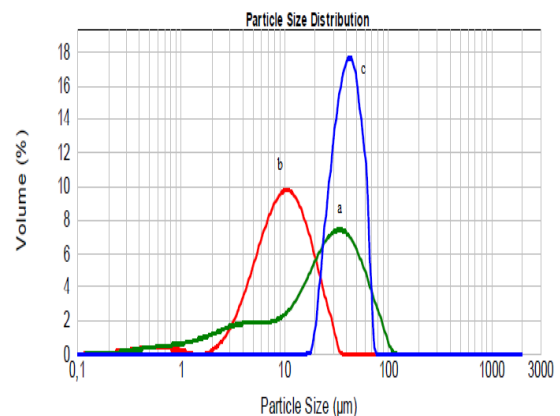


Figure 3. Particle size distribution of (a): olive pomace, (b): PANI and (c): OP/PANI Composite.

### III.1.4. Scanning electron micrographs characterization (SEM)

The percolation limiting the composite is related to the homogeneity of the mixture of the constituents. The above results can be explained according to the composite morphology, based on the characterization by SEM microscopy. Different images were taken. Fig. 4 shows an image resulting from SEM-microscopy method. In this image, the spectra (a) of olive

olive pomace, shows heterogeneous size distribution. Particle geometry is variable. Thus we observe the emergence of apparently well-crystallized grains coexisting with fine powder clusters. For the spectra (b) of PANI, there is a heterogeneous size and form of particles of PANI, as it establishes the existence of a cylindrical form with a smooth surface. This spectrum (c) shows typical SEM images of the surface of the OP/ PANI composite. We note an apparent uniformity of the surface which leaves us assume that our adsorbent is homogeneous. Also there is an increase in the size of the particle and some resemblance in the form and smoothness of the surface in comparison with the SEM images of PANI and those of composite. This confirms the results obtained by analysis of Infrared indicate that PANI was able to bind to the surface of olive pomace [29].

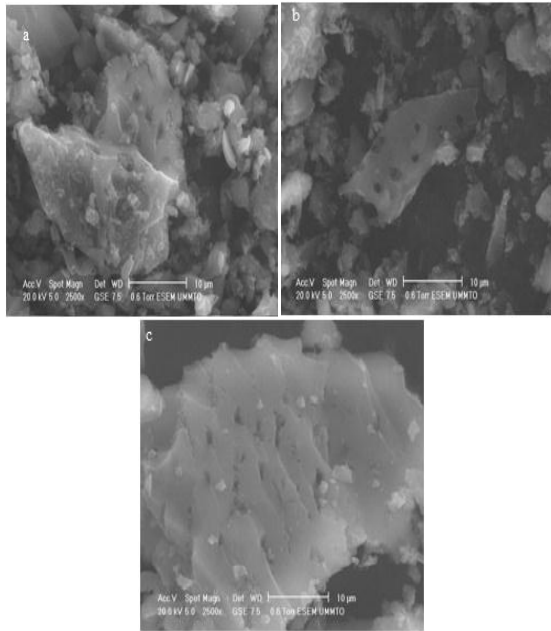


Figure 4. Scanning electron micrographs of (a) olive pomace (b) polyaniline, and (c) PO/PANI composite.

### III.2. Electrical analysis

#### III.2.1. The electrical conductivity (EC) caractérisation (four point method)

The electrical conductivity parameter was measured in the case of PANI and the PO/PANI composite prepared with different percentages of PANI, the results are shown in tables 02 and 03 respectively

Table 2: values of electrical conductivity of the PANI-HCL:

Sample	e (mm)	I (µA)	V (volt)	Resistivity (Ohm.cm)	conductivity (S/cm)
PANI	0.53	1.989	1.20.10 <sup>-4</sup>	14.4851	6.90.10 <sup>-2</sup>

The value of the conductivity obtained ( $\sigma = 0.06$  S/cm) for the synthesized polyaniline, is close to that

given in the literature, taking into account the same operating conditions.

Table 3: values of conductivity of OP/PANI-HCL composite

% PANI	$\sigma$ (S/cm)	Log $\sigma$ (S/cm)
4.63	1.23.10 <sup>-4</sup>	-3.91
8.23	1.02.10 <sup>-3</sup>	-2.99
19.18	1.5.10 <sup>-3</sup>	-2.82
23.23	2.13.10 <sup>-3</sup>	-2.82
28.15	8.81.10 <sup>-3</sup>	-2.05
39.42	3.20.10 <sup>-2</sup>	-1.49

According to the results found, we note that the insertion of the polyaniline in the olive pomace by the method of in-situ polymerization, confers a conducting appearance. Even low-PANI, composites already express a conductivity of about 1,23.10<sup>-4</sup> S/cm. The samples percolation threshold is observed in the range [25%, 40%] by weight of PANI; it reflects the formation of conjugated system.

### III.3. Electrosorption behavior

Batch mode electrosorption experiments were performed to investigate the application of the electrosorption process for the removal of chromium (VI) from aqueous solutions, using an Olive pomace-PANI composite with an (PO/PANI) electrode. The exact speciation of the chromium ions depends upon pH, temperature, concentration and the presence of other ions. However according to different authors [30,31], the Cr (VI) is in the form of  $\text{HCrO}_4^-$ ,  $\text{CrO}_4^{2-}$ , or  $\text{Cr}_2\text{O}_7^{2-}$ . The Cr (VI) forms would be drawn to the anode. Since these ions are already in a high oxidation state, complexation at the anode, without anodic oxidation is expected. To this effect we apply a positive polarization (anodic potential) to promote electrosorption chromium Cr (VI). In order to efficiently investigate on the relation between the developed conductor material (Olive pomace-PANI composite) and the effect of the electrochemical polarization on the adsorption rate (which is necessary for the accurate design and modelling of adsorption processes), an experiment on adsorption/electrosorption kinetics were carried out starting with the same initial chromium salt concentration of about 20 mg/l of chromium (VI) with an electrode area of 13.2 cm<sup>2</sup> at room temperature and recorded the adsorption at open circuit (OC) and electrosorption under 800 mv polarization as shown in Fig.5.

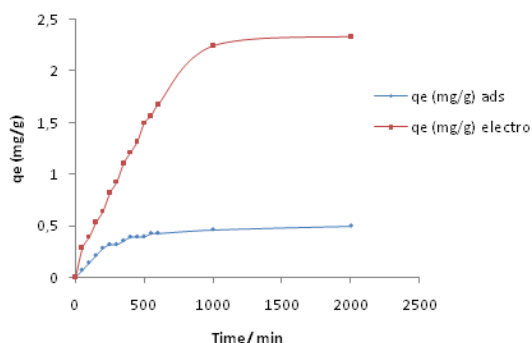


**Figure 5.** Adsorption kinetics at open circuit (OC) and electrosorption under 800 mV polarization at  $C_0$ : 20 mg/L, T: 25°C, pH: 2.6.

In order to determine the capacity for electrosorption and regenerability after electrosorption on Olive pomace-PANI composite we have carried another experiment. In this latter, the electrosorption run from adsorbate solution according to desorption run. The electrosorption data were recorded upon polarization by applying -400 mV for the first 10000 s followed by electrodesorption upon polarization by applying +400mV for the next 1200 s for the possible regeneration of Olive pomace-PANI composite. Then polarization direction was reversed in order to observe the electrosorption. The results are shown in Fig.6.

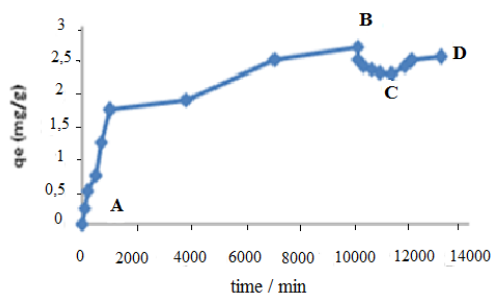


**Figure 6.** Successive electrosorption/electrodesorption (from A to D), electrosorption (from A to B) at +400mV, electrodesorption (from B to C) at -400 mV polarization, and electrosorption (from C to D); mass of OP/PANIElectrode was 0.2g.

The electrosorption takes place from A to B upon +400 mV. A decrease is observed in solution concentration of chromium, resulting in electrosorption of almost 25% of chromium in the first 10000s. When the polarization direction is reversed (-400mV) at point B to C during 1200 s as shown in Fig6, a small amount of Cr (VI) was released during this step. During regeneration step at - 400 mV polarisation, an amount of 0,5 mg g<sup>-1</sup> of electrosorbed chromium was electrodesorbed into 800ml of K<sub>2</sub>Cr<sub>2</sub>O<sub>7</sub> solution in 20 min period, corresponding to about 18,5% of the amount of

chromium electrosorbed. The remainder is absorbed. A reverse polarization at -1.2 V was required for the partial release of bound Cr (VI). This electrosorptive behavior of chromium not only can be linked to the electrostatic interactions between Chromium species in solution and charged Olive pomace-PANI composite surface in the double layer but also chemical complexation between the dichromate oxyanions with functional groups on the Olive pomace-PANI composite surface, where the relative irreversibility Cr(VI) electrosorption. It is evident that Cr(VI) anions such as dichromate are not removed from the solution by a simple electrostatic (capacitive charging) mechanism. The electrosorption process involves some type of bond formation. Reverse polarization at -400 mV caused cathodic reduction at the electrode complexed with the Cr(VI) species, thereby destroying the Olive pomace-PANI composite Cr(VI) bonds. After the regeneration, the polarization direction is reversed (+ 400 mV) at point C, the concentration starts to decrease sharply as a result of electrosorption of chromium. However, the adsorbed amount is similar that previously regenerated.

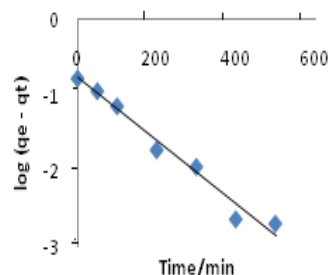
#### III.4. Comparison of electrosorption with adsorption:

Evaluation of adsorption kinetics is carried out using pseudo-first - order, and intraparticle diffusion models [32, 33].

Lagergren pseudo-first order is expressed as:

$$\log (q_e - q_t) = \log q_e - (K_1/2.303)t \quad (1)$$

Where  $q_e$  and  $q_t$  (mg/g) are the amounts of chromium adsorbent per unit mass of Olive pomace-PANI composite at equilibrium and at time  $t$ , respectively, and  $K_1$  (min<sup>-1</sup>) is the rate constant for pseudo-first-order adsorption. The values of  $K_1$  and  $q_e$  at different concentrations can be determined from the slope and intercept when  $\log (q_e - q_t)$  is plotted against  $t$  (Fig.7(a) and (b)).





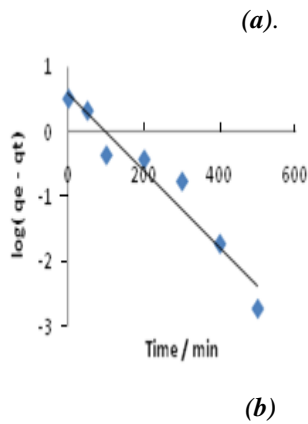


**Figure 7.** pseudo-first – order plots for adsorption :  
 (a). under potential condition at 800 mV polarization, (b).at open electroadsorption circuit (OC)

The rate constants,  $k_1$ , and corresponding regression coefficients,  $r$ , are given in (Table 4) for adsorption at open circuit (OC) and electroadsorption under potential condition at 800 mV polarization.

**Table 4.** Kinetic parameters of the removal of chromium by adsorption at open circuit and electroadsorption under potential condition at 800 mV polarization.

	Adsorption (Open circuit)	electroadsorption
Pseudo-first order		
$K_1$ ( $\text{min}^{-1}$ )	0.0092	0.0138
$q_e$ (mg/g)	0.465	1.79
$r^2$	0.976	0.940
% $R_{eq}$	18.7	86
Intraparticle diffusion		
$K_{id}$ ( $\text{mg g}^{-1} \text{min}^{1/2}$ )	0.024	0.243
$K_{2id}$ ( $\text{mg g}^{-1} \text{min}^{1/2}$ )	0.02	0.051

Positive polarization causes an increase in the rate of adsorption, and equilibrium adsorption capacities compared to open circuit adsorption; 33% increase was observed in rate constant ( $k_1$ ) and upon +800 mV polarization. This result suggesting an effect of electrostatic interactions by attraction between positively charged of Olive pomace-PANI composite and negatively charged chromium ions which is in the anionic form  $\text{Cr}_2\text{O}_7^{2-}$  and also dispersion forces are responsible from the observed enhancement in rate parameter. The intraparticle diffusion model has also been used as a first approach for identifying the limiting adsorption step and the diffusion/transport mechanisms during Chromium adsorption and electroadsorption. The intraparticle diffusion model can be represented with equation (2)

$$qt = k_{id} t^{(1/2)} + C_i(2)$$

Where  $k_{id}$  ( $\text{mg g}^{-1} \text{min}^{-1/2}$ ) is the measure of diffusion coefficient and  $C_i$  ( $\text{mg g}^{-1}$ ) is the intraparticle diffusion constant which is directly proportional to the boundary layer thickness. The diffusion plots of  $qt$  vs.  $t^{(1/2)}$  gives the rate constant,  $K_{id}$  from the slope and  $C_i$  from the intercept. The multi-linear nature of the intraparticle diffusion plots (two differentiated steps were detected in adsorption and electroadsorption) indicates the simultaneous occurrence of several adsorption stages.

The first linear step represents the adsorbate diffusion in the boundary layer; the second one accounts for the gradual adsorption stage where the molecules of the adsorbate diffuse through the porosity of the composite electrode (intraparticle diffusion). Fig 8(a) and (b) presents respectively the plots of chromium electroadsorption upon polarization by applied potential of the order of 800 mV and open circuit (OC) versus  $t^{1/2}$  on Olive pomace-PANI composite. It can be seen from the figure that data points are linked by two straight lines.

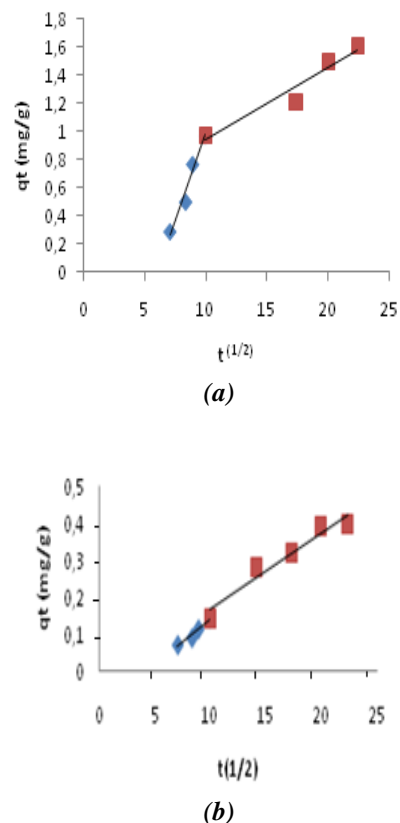


**Figure 8.** Intraparticle diffusion plots:  
 a). for the Electroadsorption upon polarization by applying Potential of the order of 800 mV.  
 b). for the adsorption at open circuit (OC).

For the electroadsorption upon polarization by applying potential of the order of 800 mV, the external mass

transfert step occurring at low contact times during the retention of chromium was further explored by determining the rate constant of external mass transfer  $K_{1id}$  (diffusion in the boundary layer) from the initial period of adsorption. The second distinctive linear region marks the stage where intraparticle diffusion starts controlling the rate of adsorption ( $K_{2id}$ ).  $K_{1id}$  and  $K_{2id}$  are included in Table 2. It is clear the intraparticle diffusion ( $K_{2id}$ ) is slower than the external mass transfer (diffusion in the boundary layer). This indicates that the external mass transfer is not the rate-controlling step for electroadsorption of chromium. Our results are similar of the work concerning electroadsorption of basic dyes and pyridine from aqueous solution onto activated carbon cloth electrode [35]; showing that this electroadsorption is not diffusion controlled in the boundary layer. Whereas for the open circuit (OC) adsorption, we see that the rate of constant for the external mass transfer step and the intraparticle diffusion are the same (table 4). However, the intercepts of the plots do not pass through the origin. This indicates that intraparticle diffusion is not the only rate limiting step, but also other kinetic models may control the rate of adsorption [32]. The rate limiting step maybe a complex combination of chemisorption and intraparticle transport [32] (Table 4).

#### IV. Conclusion

In the present paper, Olive Pomace /PANI conductive composites were prepared by chemical oxidative polymerization of aniline with natural olive pomace. The FT-IR spectrum of OP/PANI indicates that the compositing of OP and PANI is successful. On the other hand, XRD of OP/PANI-HCl composite reveals broad diffraction peaks typical to those obtained from the pure PANI and the pure olive pomace indicating a successful coating of PANI over olive pomace.

Agglomeration between particles of Olive Pomace and PANI is determined by The Laser granulometry which indicates that after mixing; there was an increase in particle size.

Scanning electron micrographs characterization (SEM) confirms results obtained by FT-IR and DRX Laser granulometry analysis. These results indicate that the PANI is successfully fixed on the OP.

The conductive composite was used in the chemical and electrochemical removal of Cr(VI) from aqueous solutions. The Cr(VI) is in the form of  $\text{HCrO}_4^-$ ,  $\text{CrO}_4^{2-}$ , or  $\text{Cr}_2\text{O}_7^{2-}$ , they would be drawn to the anode. Since these ions are already in a high oxidation state, complexation at the anode, without anodic oxidation is expected. To this effect we apply a positive polarization (anodic potential) to promote electroadsorption chromium Cr(VI). An experiment

was carried out in which electroadsorption run from adsorbate solution were followed by an desorption run indicating that this electroadsorption behavior of chromium can also be linked to the chemical complexation between the dichromate oxyanions with functional groups on the Olive pomace-PANI composite surface. Finally, the kinetic data are fitted well with the pseudo-first-order model and intraparticles diffusion model

#### V. References

1. Randall, J. M.; and Hautala, E. Removal of heavy metal ions from waste solutions by contact with agricultural by products. *Proceeding. Industry. Waste conference*. 30 (1975) 412 – 422.
2. Pagnanelli, F.; Maielli, S.; Veglio, F.; and Toro, L. Heavy metal removal by olive pomace: biosorbent characterisation and equilibrium modelling. *Chemical Engineering Science* 58 (2003) 4709 – 4717.
3. Ayranci, E.; and Conway, B. E. Adsorption and electroadsorption at high-area carbon-felt electrodes for water purification: systems evaluation with inorganic, S-containing anions. *Journal of Applied Electrochemistry* 31 (2001) 257-266.
4. Bayram, E.; Ayranci, E. Electrochemically enhanced removal of polycyclic aromatic basic dyes from dilute aqueous solutions by activated carbon cloth electrodes. *Environmental. Science and Technology* 44 (2010) 6331-6336.
5. Ania, C. O.; Béguin, F. Mechanism of adsorption and electroadsorption of bentazone on activated carbon cloth in aqueous solutions. *Water Research* 41 (2007) 3372-3380.
6. Ramirez-Garcia, S.; Cespedes, F.; Alegret, S. *Electroanalysis*. 13 (2001) 529.
7. Prabakar, S. J. R.; Narayanan, S. S. *Talanta* 72 (2007) 1818.
8. Casado, U. M.; Aranguren, M. I.; and Marcovich, N. E. Preparation and characterization of conductive nanostructured particles based on polyaniline and cellulose nanofibers. *Ultrasonics Sono chemistry* 21 (2014) 1641-1648.
9. Babakhouya, N.; Boughrara, S.; and Abad, F. Kinetics and thermodynamics of Cd(II) ions sorption on mixed sorbents Prepared from Olive Stone and Date pits from Aqueous Solution. *American Journal of Environmental Sciences* 6 (5) (2010) 470-476.
10. Hu, W.; Chen, S.; Yang, Z.; Liu, L.; and Wang, H. Flexible electrically conductive nanocomposite membrane based on bacterial cellulose and polyaniline. *The journal of physical chemistry. B* 115 (2011) 8453-8457.
11. Li, S.; Huang, D.; Zhang, B.; Xu, X.; Wang, M.; Yang, G.; and Shen, Y. Flexible Supercapacitors Based on Bacterial Cellulose Paper Electrodes. *Advanced Energy Materials*. (2014) 1.301- 655.
12. Tazibet, S.; Boucheffa, Y.; Lodewyckx, P.; Velasco, L. F.; Boutillaraa, Y. Evidence for the effect of the cooling down step on activated carbon adsorption

- properties. *Microporous and Mesoporous Materials* 221 (2016) 67-75.
13. Lamouri et al. The Preparation and Analytical Study of Conducting Polyaniline Thin Films. *Journal of Petroleum Environmental Biotechnology*. 2014, 5:2.
  14. Adams, P.N.; Laughlin, P. J.; Monkman, A. P.; and Kenwright, A. M. *Polymer*. 37 (1996), 3411.
  15. Zun-li Mo, Zhong-li Zhao, Hong Chen, Gui-ping Niu, and Hua-feng Shi. Heterogeneous preparation of cellulose-polyaniline conductive composites with cellulose activated by acids and its electrical properties. *Carbohydrate Polymers*. 75 (2009), 660-664.
  16. Sheimann, F. An introduction to spectroscopic methods for the identification of organic compounds. *Pergamon Press*, 1998.
  17. Bellamy, L. J. The infrared spectra of complex molecules. *Chapman and Hall, London*, Vol. 1 (1975).
  18. Hesse, M.; Meir, H.; and Zeeh, B. Méthodes Spectroscopiques pour la chimie organique. *Masson, Paris*. (1997).
  19. Xuan Z.; and Lu, L. *Mater. Lett.* 65 (2011) 754-756.
  20. Ayad, M.; El-Hefnawy G.; and Zaghlol, S. *Chemical Engineering Journal* 217 (2013) 460-465.
  21. Malkoc, E. Adsorption of chromium (VI) on pomace—An olive oil industry waste: Batch and column studies. *Journal of Hazardous Materials*. (2006) 142–151.
  22. DjalalTrache, André Donnot, KamelKhimeche, RiadBenelmir, and Nicolas Brosse. Physico-chemical properties and thermal stability of microcrystalline cellulose isolated from Alfa fibres. *Carbohydrate Polymers*. 104 (2014) 223–230.
  23. M.H. Schneider and K. I. Brenbner. «Wood-polymer combinations: The chemical modification of wood by alkoxysilane coupling agents.», *Wood Science Technology* 19 (1985) 67-73.
  24. F. Zhang, Z. Pang, C. Dong, Z. Liu, Preparing cationic cotton linter cellulose with high substitution degree by ultrasonic treatment, *Carbohydrate Polymers* 132 (2015) 214–220.
  25. F. Yang, M. Xu, S.-J. Bao, H. Wei, and H. Chai, Self-assembled hierarchical graphene/ polyaniline hybrid aerogels for electrochemical capacitive energy storage, *Electrochimica Acta* 137 (2014) 381–387.
  26. Kumar, M.; Singh, K.; Dhawan, S.K.; Tharanikkarasu, K.; Chung, J.S.; Kong, B.-S.; Kim, E.J.; and Hur, S.H. Synthesis and characterization of covalently-grafted graphene–polyaniline nanocomposites and its use in a supercapacitor. *Chemical Engineering Journal*. 231 (2013) 397–405.
  27. Ahmed Mekkia, Soumen Samantaa, Ajay Singh, Zakaria Salmia, Rachid Mahmoud, Mohamed M.; Chehimia1, Dinesh K. Aswalc Core/shell, protuberance-free multiwalled carbon nanotube/polyaniline nanocomposites via interfacial chemistry of aryl diazonium salts. *Journal of Colloid and Interface Science*. 418 (2014) 185–192.
  28. Dallas, P.; Moutis, N.; Devlin, E.; Niarchos, D.; and Petridis, D. *Nanotechnology* 17 (2006) 5019.
  29. De Bondt, S.; Froyen, L.; and Deruyttere, A. *Journal of Materials Science- Springer*. 27 (1992) 1983.
  30. Dana Lindsay, Kevin J Farley, Richard F. Carbonaro, Oxidation of CrIII to CrVI During Chlorination of Drinking Water, Electronic Supplementary Material (ESI) for Journal of Environmental Monitoring. *The Royal Society of Chemistry* 2012.
  31. Elisabeth L.; Hawley, Rula A.; Deeb, Michael C.; Kavanaugh and James Jacobs R.G. *Treatment Technologies for Chromium (VI)*. (2004), 273.
  32. Mukoko, T.; Mupa, M.; Guyo, U.; Dziike, F. Preparation of Rice Hull Activated Carbon for the Removal of Selected Pharmaceutical Waste Compounds in Hospital Effluent. *J Environ Anal Toxicol* (2015) doi:10.4172/2161-0525.S7-008.
  33. Karthikeyan T.; et al., *Journal of Hazardous Materials*. 124 (2005) 192 – 199.
  34. Jonathan Febrianto et al. Equilibrium and kinetic studies in adsorption of heavy metals using biosorbent: A summary of recent studies. *Journal of Hazardous materials* 162 (2009) 616 – 645.
  35. Edip Bayram, Erol Ayranci. Investigation of changes in properties of activated carbon cloth upon polarization and of electrosorption of the dye basic blue-7. *Carbon* . 48, (2010) 1718–1730.



**Please cite this Article as:**

Babakhouya.N, Abdouni. M, Louhab .K, Preparation and characterization study of an olive pomace - polyaniline composite conductor in the recovery of heavy metals by electrosorption and adsorption., *Algerian J. Env. Sc. Technology*, 4:2 (2018) 18-25